Revealing the Penfield Map with functional MRI data

Olusanmi Hundogan
Utrecht University

This paper explores the results of the famous cortical homunculus discovered by Penfield and Boldrey in 1937 . The model shows the representation of various body parts in the cerebral cortex. While Penfield used medical insights to deduce his results, this paper will further cement the validity with bio-electric imaging techniques like fMRI, which have a higher spatial resolution.

Keywords: neuroscience, fMRI, analysis, basic, brain, cortical homunculus, parietal lobe, cerebral cortex

Introduction

In 1937 the scientists Penfield and Boldrey provided a scientific basis for something that humans intuitively understood for millennia: Not all body parts are created equal; some of them are more important than others. In a series of experiments, he used cortical stimulations and patient responses to construct a map for sensory and motoric functions in brain regions[9]. These experiments were highly invasive and became obsolete because we have access to non-invasive imaging techniques such as fMRI. These technologies can tell us more about the functional responsibilities of different brain tissues. These techniques are by no means perfect[2] but remain very informative. In this paper we will showcase the sustained relevance of Penfield and Rasmussen's map, by showing activations in fMR-data that align with Figure 1 [10]. The figure shows how motoric functions are distributed across the primary motor and somatosensory cortex. In the axial perspective we should also see the activation of both hands in contralateral hemispheres of the cortex as described by Dassonville et al.[4].

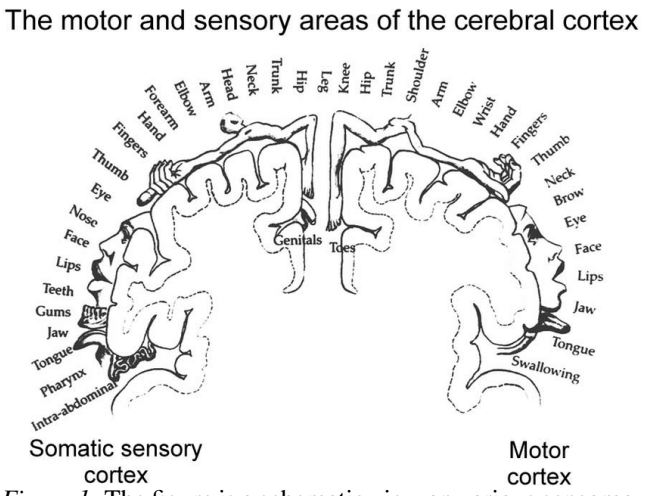

Figure 1. The figure is a schematic view on various sensomotoric functions as they were originally specified by Penfield and Rasmussen in 1950

Methods

Participants

This analysis incorporated the fMRI data of 18 participants. Each participant went through a series of tasks. These tasks included motoric- (feet, left hand, right hand, tongue), working-memory-, verb-generation- and picture-naming tasks. For this analysis, we will only consider the neural data of the motoric tasks.

Procedure

The participants were instructed to execute a motoric task upon perceiving visual stimuli. Each task was conducted in a separate session and contains movements for *both feet together*, the *left hand*(LH), the *right hand*(RH) and the *tongue*. We ran a preprocessing pipeline for each subject, described in section and Figure 2 in greater detail. Furthermore, each motoric task was handled as a separate session. This separation simplifies the preprocessing pipeline concerning subject-specific corrections. The analysis uses fMRI scanning sequences with a repetition time (TR) per time unit of 2.5. The tasks were conducted as event-related experiments which alternated between blocks of control conditions and stimulus conditions. The onset times differed for every task but lasted roughly 30 seconds on average.

Materials

The analysis uses SPM 12 for the preprocessing and statistical analysis of the data. The visualizations were generated using Python 3.7.7 and the Nilearn 0.7.1 library. The calculations were run on an i7-9750H processor with 2.6GHz and

32GB RAM. The operating system was Windows 10 Home x64 Version 20H2.

Results

Preprocessing

The preprocessing pipeline starts by realigning and reslicing the data to correct within-subject differences of head positions. For each session and subject, the realignment is estimated using a quality level of 0.9 with a sampling resolution of 2.5mm and a 5mm smoothing kernel. The number of passes required twice the time as the results were registered to the mean. The interpolation was kept at the 2nd degree for the estimation and the 4th degree during the writing of the slices. Figure 2 shows the results of the realignment procedure. It shows the most vital adjustment in the y-translation with a clear drift over the slices. For rotation adjustments, rx appears to contain the most variance, while ry and rz remain relatively stable. If we focus on each condition, the Feet- and to lesser extent Tongue-condititions show sinusoidal behaviours.

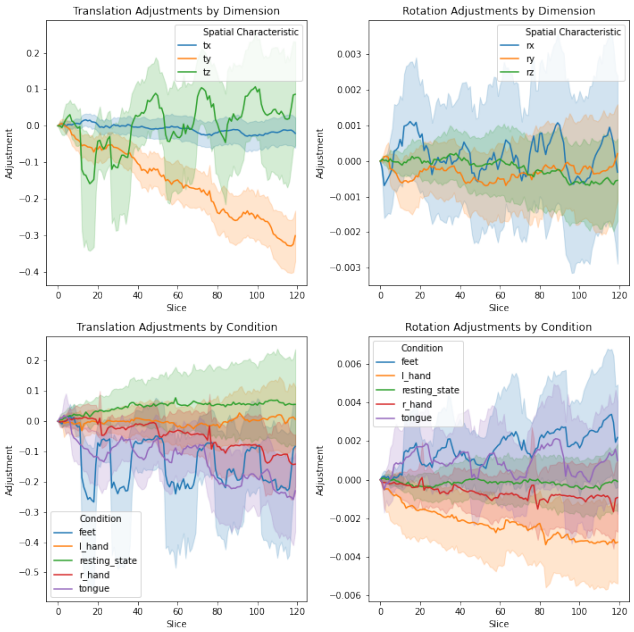

Figure 2. The figure displays the results of the realignment step. We omit the confidence interval for better visibility. The figure shows the adjustments by task condition (feet, left hand (LH), right hand (RH) and tongue) and spatial characteristic (translation and rotation). Translations were originally measured in mm and rotations in degrees.

This behaviour is likely caused by the alternating movements for both conditions. This notion is further supported by Figure 3. Here, we can see a strong adjustment for every onset time for the duration of the condition. Hence, we have to consider that the data is subject to strong movement-related confounds. As the data is interleaved and the motoric

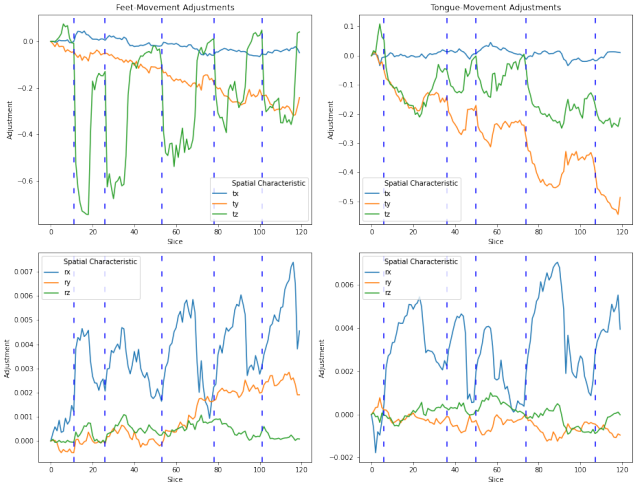

Figure 3. The figure shows the results of the realignment step for Feet- and Tongue-movements. The confidence intervals cover 95%. Translations were originally measured in mm and rotations in degrees. The dashed lines show stimulus onsets.

tasks may yield strong head motions, the slices will not be time-corrected. In Figure 5 we show how the feet-movement condition suffers severely from artifacts.

Apart from realigning and reslicing, the preprocessing pipeline also coregistered each slice towards the anatomical image. The reference image is the mean across all slices. The mean image yields the least noise and, therefore, acts as the most appropriate choice. Furthermore, we will use the *Normalised Mutual Information* as an objective function. Lastly, we will apply a Gaussian smoothing for the joint histogram. This approach prevents artefacts like holes that typically arise from sharp binning and precise histogram binning. We will use a 7x7 kernel for this procedure.

Afterwards, we normalize T1 and use the resulting deformation field to warp the functional images concerning the standard tissue probability map provided by SPM. The estimation uses a sampling rate of 2, and for the warping process, we write voxels that are sized according to the acquired voxel sizes *(2.9mm x 2.9mm x 3mm)*.

At last, we smooth the images to account for inaccuracies after the normalization. Here, we chose the settings recommended by the SPM manual [1] which entails using a 6x6x6mm kernel.

The results of each processing step are seen in Figure 4.

First-Level Analysis

For the first-level analysis, we fit a general linear model with additional regressors for motion parameters and HRF time and dispersion correction. Additionally, we add a high

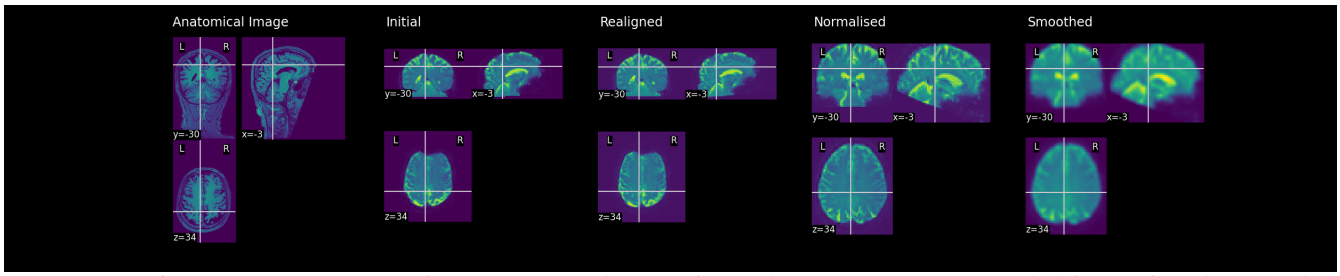

Figure 4. The figure shows the results of each preprocessing step for Subject 1. The steps are applied from left to right, starting from the in initial image. For each axis we show three slices.

pass filter to account for frequency drifts in the data. We also reduce the masking threshold to 0.5 as 0.8 (SPM-default) was deemed too high. Lastly, we include the resting state in the model without condition in the model. This resulted in 59 beta maps. For the contrasts, we mainly model the following contrast groups...

Grp-1: the increase of each condition with the resting state (5 contrasts: [1], [0 1], [0 0 1], etc.)

Grp-2: the increase against all other conditions without the resting state (4 contrasts: [3 -1 -1 -1], [-1 3 -1 -1])

Grp-3: a contrast for each hand against the opposite hand (2 contrasts: [1 -1] and [-1 1])

Grp-4: the activation of all conditions (1 contrast: [1 1 1 1])

Grp-5: the average and contrasted increase of both hands together against the other conditions (2 contrasts: [0 1 1 0] and [-1 1 1 -1])

These contrasts focus on increasing neural activation, as they align with the insights one can receive with crude invasive procedures as conducted by Penfield and Boldrey. Hence, deactivation patterns are not further considered. Figure 5 shows a set of 6 subject brains from a sagittal perspective. Each row represents one condition (feet, LH, RH and tongue) which contrasts with every other condition (Grp-2). This approach implicitly masks interaction effects as we only concentrate on one condition at a time for our statistical analysis. Therefore, we will focus on these contrasts primarily.

The aforementioned Figure 5 hints at a strong activation for left-hand movements in the *right pre-and postcentral gyrus of the motor cortex*. We also see activations in the *occipital lope* for some subjects. The occipital lobe is generally associated with visual processing. Therefore, we assume it is related to the visual stimuli. Similar holds for right-hand movement with activation on the left hemisphere; albeit, much weaker. Intuitively, this one-sided bias is reasonable as most people predominately use their right hand for most tasks. Hence, the enhanced activation for the left hand may go hand in hand with higher coordination efforts for the less dominant hand. However, these remarks require a more thorough investigation.

Before proceeding with the second-level analysis, it will be necessary to address a possible detriment in the data. After the first-level analysis, the beta-maps of several images for several subjects revealed artefacts across the image. The artefacts have the shape of stripes in their sagittal and coronal view. Although this effect occasionally occurs for some subjects, Figure 6 shows how these artefacts predominantly arise for the feet-condition (see the first row in comparison). This phenomenon hints at issues related to subject movements. Another possibility could be measurements errors during data acquisition, as this issue appears to be expected for this dataset. The issues could be mitigated by either unwarping the data for strong head movements or an additional regressor trying to capture the signal. However, as these artefacts' influence does not interfere with this paper's target, we did not enact any further measures. In simple terms, we can ignore the artefacts, as they cancel out during the statistical tests during the second-level analysis.

Second-Level Analysis

After the first-level analysis, we conduct a one-sample t-test for each contrast. We chose an FWE of 0.01 as a significance level. Furthermore, we define a region of interest by masking the results across the Brodmann Areas 1-7. These areas cover the primary motor and somatosensory cortex. Without the masking procedure, we also see activations in the occipital lobe, which overshadow the tongue activations (see. Appendix D). To visually inspect the results, we first show 15 coronal slices and contours of significant activations in Figure 7.

The figure clearly shows the activation of the feet (green), the LH (red), the RH (cyan) and the tongue (magenta) across the *parietal lope*. Table 1 holds the significance values of the most prominent cluster for each condition. The table also includes hand comparisons. In sum, the average increase for every condition returns ten significant clusters with $p < 0.001$ and a height threshold of $T = 6.82$ across the parietal lobe. The left-hand movement shows the highest contrast to all other movements. This effect is reasonable if we con-

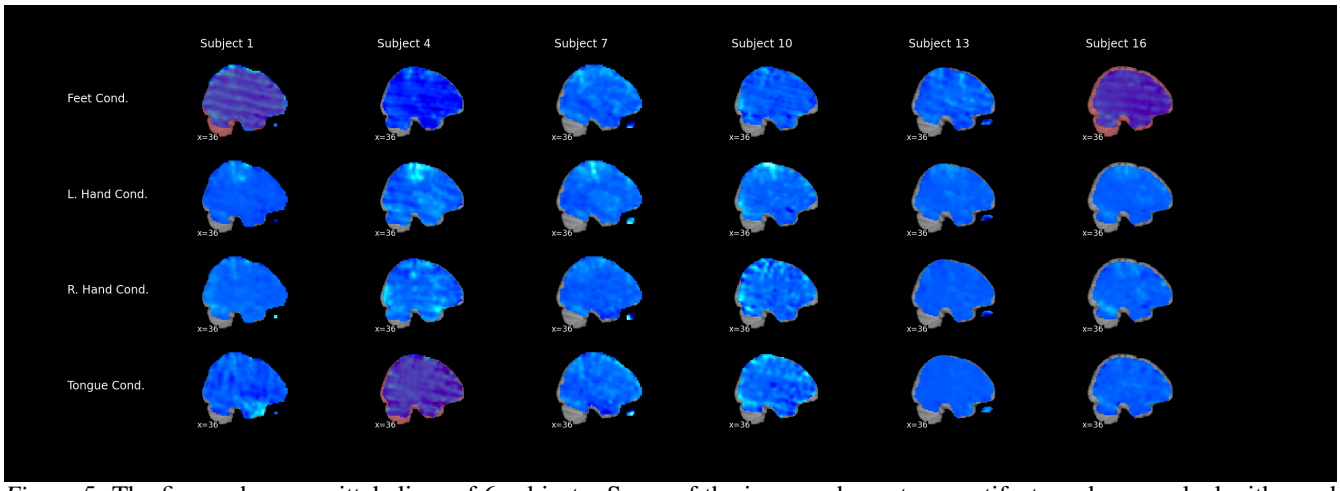

Figure 5. The figure shows sagittal slices of 6 subjects. Some of the images show strong artifacts and are marked with a red overlay. Furthermore, areas in the occipital and perietal lope show activity.

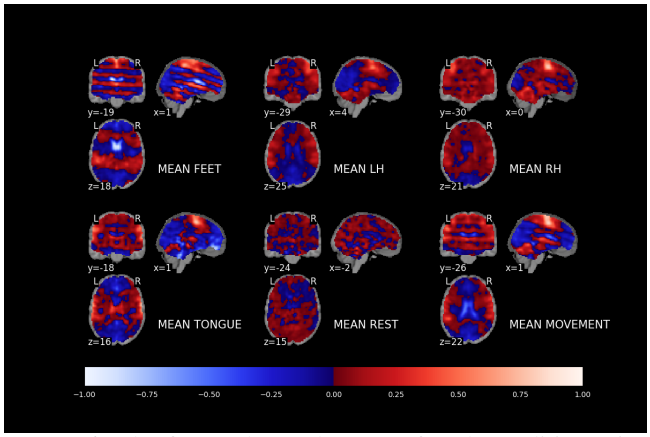

Figure 6. The figure shows the cuts of each conditions significant slices as a mean accross each subject. It shows how prevalent the artifacts are in the feet condition. The average movement shows similar pattern caused as it includes feet movements.

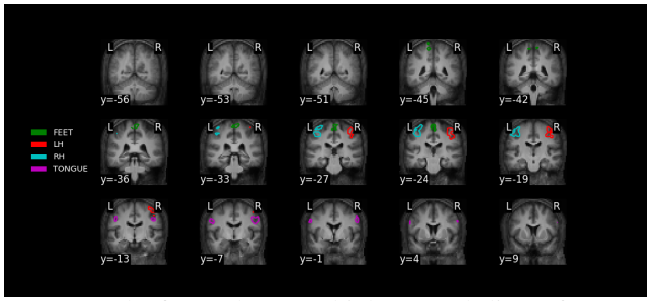

Figure 7. The figure shows multiple coronal slices of a mean anatomical image. Each contour represents a different task condition. The color mapping is as follows: (feet = green), (LH = red), (RH = cyan) and (tongue = magenta). We thresholded the T-maps at their 99.9 percentile.

sider that difficult tasks require more cognitive resources, and left-hand movements are more difficult for right-handed people. Most people are right-handed. Another noteworthy observation is the unilateral strength of the Tongue condition in the right hemisphere. Again, reminiscent of the dominance of one hemisphere in the brain. We also tested for the effects of the HRF time and dispersion regressors. However, they did not show any significance below 0.05 for FWE. Same holds for each derivative-regressor on its own. On the other hand, every cluster we present in Table 1 remains significant if contrasted with those additional derivatives. Interestingly, every condition except the feet condition (FWE > 0.05 for all clusters) shows a significant difference, if contrasted with dispersion. Furthermore, the RH condition shows significance, but it appears weak ($P_{FWE-corr}$0.002, $k_E = 5$, $T = 6.33$, $Z = 4.48$, $coord = (-35, -22, 53)$. However, the cluster location remains on the contra-lateral side of the LH respective cluster ($P_{FWE-corr} < 0.000$, $k_E = 18$, $T = 6.82$, $Z = 4.67$, $coord = (37, -22, 53)$. Therefore, these activations are unlikely false-positives but rather due to the imbalance of left-handed subjects. We see a similar pattern for the difference between the condition and time-HRF regressor. This time, the feet condition remains largely unaffected ($P_{FWE-corr} < 0.000$, $k_E = 71$, $T = 8.51$, $Z = 5.25$, $coord = (8, -8, 68)$. On the contrary, Tongue movements only show a significance for one cluster consisting of three voxels ($P_{FWE-corr} < 0.007$, $k_E = 3$, $T = 6.14$, $Z = 4.40$, $coord = (-53, -5, 29)$ and a fairly high $FDR = 0.144$.

Appendix A shows each significant region and a contour of the corresponding region according to the *Harvard-Oxford* atlas[7]. Here, we can observe an activity increase for each condition at *the pre- and postcentral gyrus*. Furthermore, the

	$P_{FWE-corr}$	$P_{FDR-corr}$	k_E	P_{uncorr}	T	Z	Location (x,y,z)
Cond. vs. Rest ($FWE < 0.01$)							
Feet	<0.001	<0.001	19	<0.001	9.02	5.39	(-3, -31, 65)
Left Hand	<0.001	<0.001	206	<0.001	16.75	6.90	(43, -28, 62)
Right Hand	<0.001	<0.001	118	<0.001	14.31	6.53	(-41, -22, 59)
Tongue (l)	<0.001	<0.001	30	<0.001	8.75	5.32	(58, -5, 32)
Tongue (r)	<0.001	0.003	8	0.002	7.38	4.88	(-55, -2, 32)
LH vs. RH Hand	<0.001	<0.001	189	<0.001	14.31	6.53	(34, -22, 50)
RH vs. LH Hand	<0.001	<0.001	119	<0.001	14.05	6.49	(-35, -22, 56)
Cond. vs. Both-Deriv. ($FWE < 0.05$)							
Feet	<0.001	<0.001	60	<0.001	10.39	5.75	(0, -16, 71)
Left Hand	<0.001	<0.001	66	<0.001	8.40	5.21	(37, -22, 53)
Right Hand	<0.001	0.019	10	0.006	6.97	4.73	(-35, -22, 56)
Tongue (l)	<0.001	0.003	20	0.002	7.38	4.88	(55, -2, 32)
Tongue (r)	<0.001	0.001	19	<0.001	8.53	5.25	(-55, 1, 32)
Cond. vs. Disp.-Deriv. ($FWE < 0.05$)							
Left Hand	<0.001	0.001	18	<0.001	6.82	4.67	(37, -25, 53)
Right Hand	0.002	0.095	5	0.032	6.33	4.48	(-35, -22, 56)
Tongue (l)	<0.001	<0.000	17	<0.000	7.59	4.95	(55, 7, 32)
Tongue (r)	0.015	0.255	7	0.007	7.00	4.74	(-55, 1, 32)
Cond. vs. Temp.-Deriv. ($FWE < 0.05$)							
Feet	<0.001	<0.001	71	<0.001	8.51	5.25	(8, -8, 68)
Left Hand	<0.001	<0.001	35	<0.001	7.64	4.94	(49, -22, 53)
Right Hand	<0.001	0.212	10	0.003	7.14	4.79	(-35, -22, 56)
Tongue (r)	0.007	0.144	3	0.144	6.14	4.40	(-53, -5, 29)

Table 1
Table shows each condition and their p-values values for the biggest cluster. It also shows the T and Z values as well as the locations of cluster peaks. The Tongue has two entries as the activations appear in both hemispheres (hemispheres). Insignificant results are omitted.

figure shows again how both hand conditions are activated in opposite hemispheres (for more details on the hand conditions see Appendix B). Each of the brain regions aligns with the initial findings of Penfield and Boldrey.

Discussion

This analysis provides further evidence for the modular composition of the motoric control of body parts on the cerebral cortex. For this purpose, we analyzed the fMRI data of *18* participants. The second-level analysis of the data revealed functionally distinct areas on the cerebral cortex that can be mapped onto different movement tasks conditions.

The results largely align with the areas, that Penfield and Boldrey identified [9]. The results also support Coren and Porac results, who discovered that both cerebral hemispheres functionally act on opposite sides of the body[3]. Dassonville et al. extended his ideas by showing that the activation of the hemispheres are unequal and depend on the subjects handedness [4]. As few people are left-handed and higher activations relate to increased cognitive effort, it explains why the right hemispheres has stronger activation patterns.

Although these results may strengthen the belief in the modular constitution of the brain, it is important to acknowledge the works of Mitchell et al. The work reveals distributed patterns of representations in the brain. The distributional characteristic of brain representations may extend to motoric functions in the brain as well. Although both ideas of functional representation remain popular as opposing paradigms within neuroscience, they do not need to be mutually exclusive. Future research needs to uncover the nature of modular and distributed representations of the brain.

Conclusion

With Figure 7 we show a strong evidence for Penfield and Boldrey map's validity. Most of the significant activations occur in the primary motor and somatosensory cortex. How-

ever, it is necessary to define a ROI, as confounding elements like activations in the primary visual cortex may obscure the effects of subtle motoric movements like the tongue.

References

Ashburner, J., Csernansky, J., Davatzikos, C., Fox, N., Frisoni, G., & Thomson, P. (2003). Computer-assisted imaging to assess brain structure in healthy and diseased brains. *The Lancet Neurology*, *2*(2), 79–88. doi:10.1016/S1474-4422(03)00304-1

Catani, M. (2017). A little man of some importance. *Brain*, *140*(11), 3055–3061. doi:10 . 1093 / brain / awx270. pmid: 29088352

Coren, S., & Porac, C. (1977). Fifty centuries of right-handedness: The historical record. *Science*, *198*(4317), 631–632.

Dassonville, P., Zhu, X.-H., Ugurbil, K., Kim, S.-G., & Ashe, J. (1997). Functional activation in motor cortex reflects the direction and the degree of handedness. *Proceedings of the National Academy of Sciences*, *94*(25), 14015–14018. doi:10.1073/pnas.94.25.14015. pmid: 9391144

DESTRIEUX, C., FISCHL, B., DALE, A., & HALGREN, E. (2010). Automatic parcellation of human cortical gyri and sulci using standard anatomical nomenclature. *NeuroImage*, *53*(1), 1–15. doi:10.1016/j.neuroimage.2010.06.010. pmid: 20547229

Fischl, B., Sereno, M. I., Tootell, R. B., & Dale, A. M. (1999). High-resolution intersubject averaging and a coordinate system for the cortical surface. *Human Brain Mapping*, *8*(4), 272–284. doi:10 . 1002 / (sici) 1097-0193(1999)8:4<272::aid-hbm10>3.0.co;2-4. pmid: 10619420

Jenkinson, M., Beckmann, C., Behrens, T., Woolrich, M., & Smith, S. (2012). Fsl. *NeuroImage*, *62*(2), 782–790. doi:10.1016/j.neuroimage.2011.09.015

Mitchell, T. M., Shinkareva, S. V., Carlson, A., Chang, K.-M., Malave, V. L., Mason, R. A., & Just, M. A. (2008). Predicting human brain activity associated with the meanings of nouns. *science*, *320*(5880), 1191–1195.

Penfield, W., & Boldrey, E. (1937). Somatic motor and sensory representation in the cerebral cortex of man as studied by electrical stimulation. *Brain*, *60*(4), 389–443.

Penfield, W., & Rasmussen, T. (1950). *The cerebral cortex of man; a clinical study of localization of function*. Oxford, England: Macmillan.

Appendix A
Contours and Hemispheres

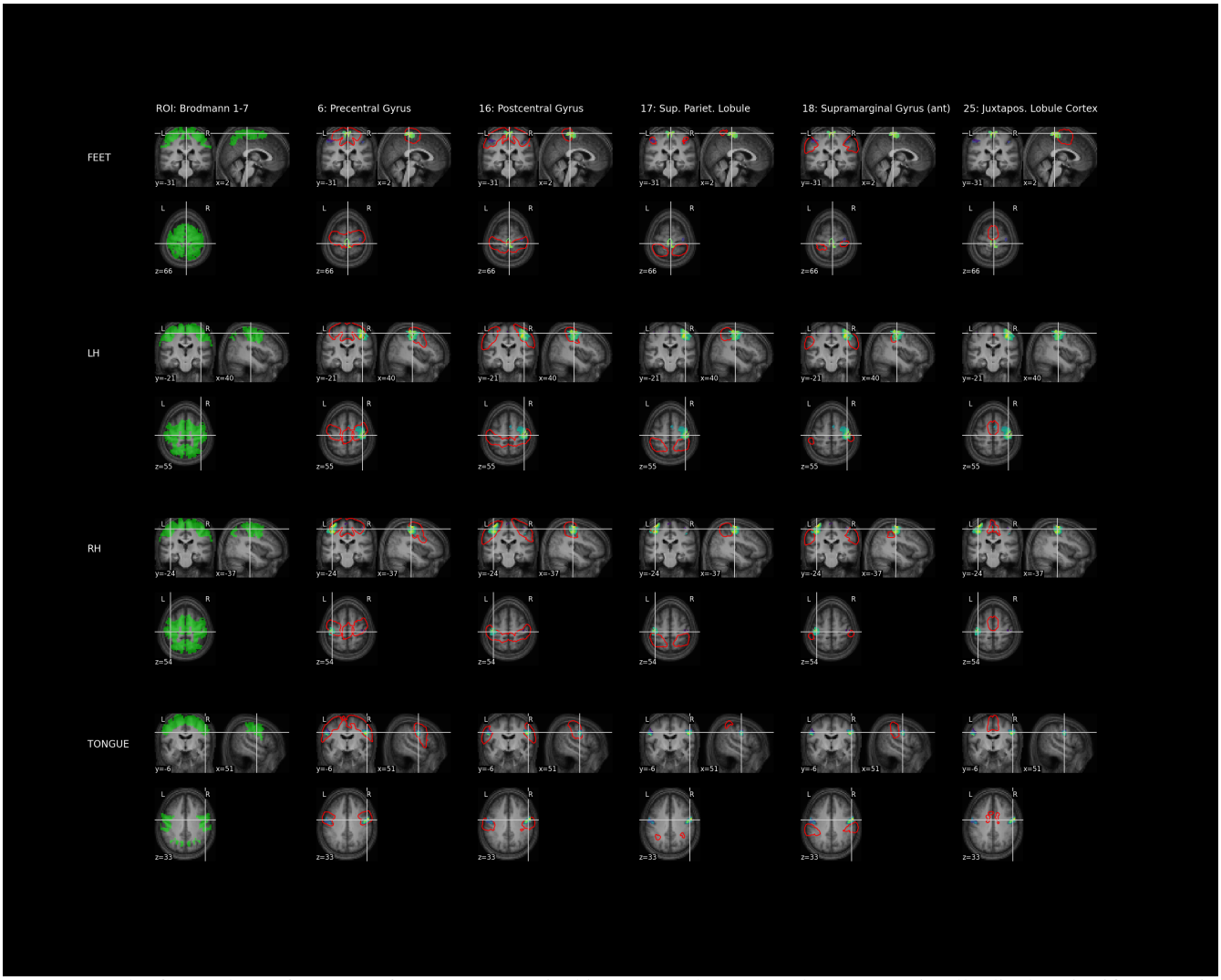

Figure A1. The figure shows four cuts of a mean anatomical image. Each cut was chosen to optimally display significant brain activation for each condition. The first column shows the ROI. The remaining images show contours of five brain areas for each cut. The figure also accounts for dispersion and time in the HRF.

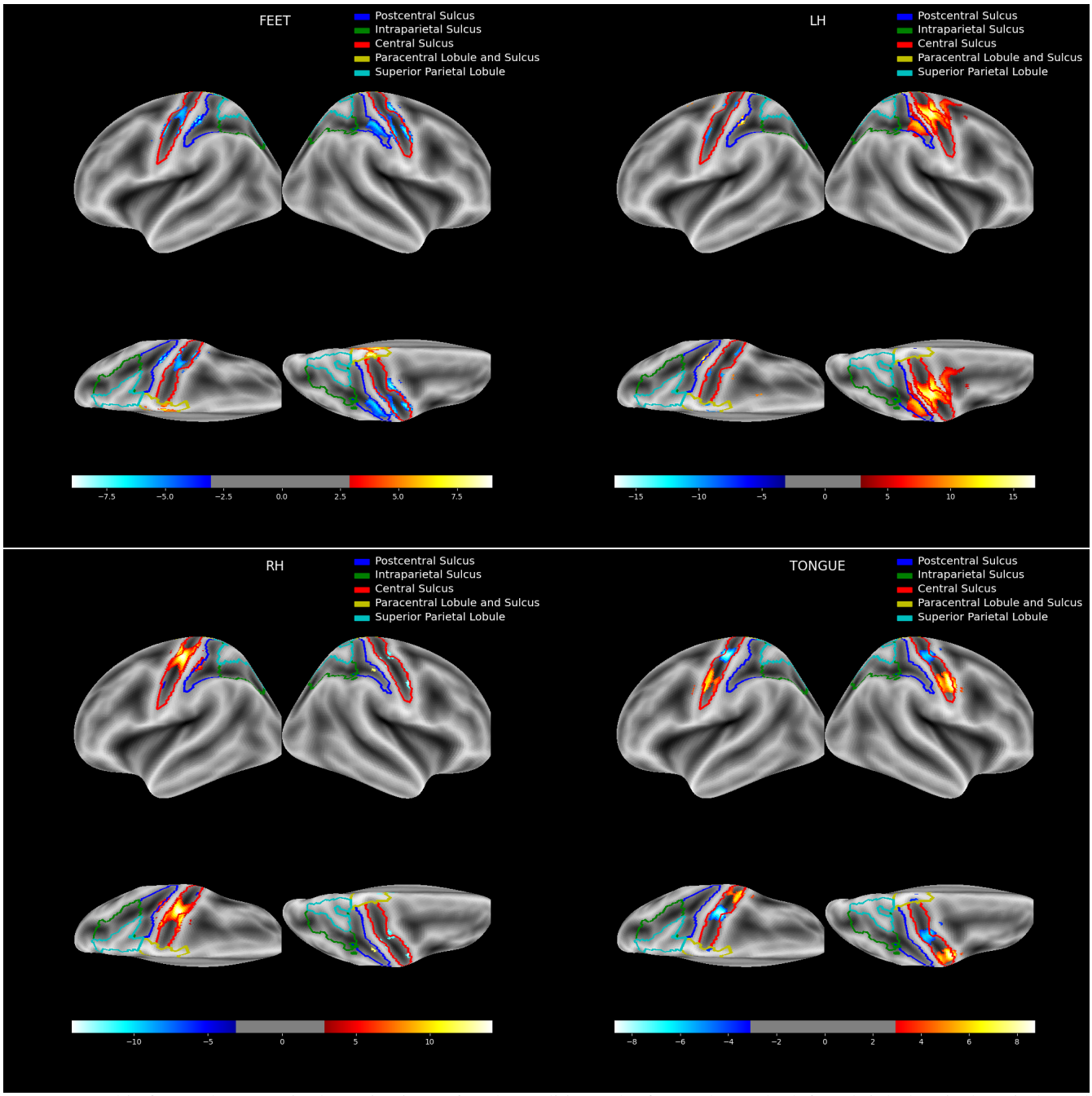

Figure A2. This figure shows again the activations of each condition. The figure shows the left and right hemisphere in lateral and dorsal view. The activations were projected on an inflated version of Fischl et al.'s average surface. This time contoured by DESTRIEUX et al.'s surface atlas. In this atlas the activations mainly appear in the sulci of the parietal lobe.

Appendix B
Left and Right Hand Movements

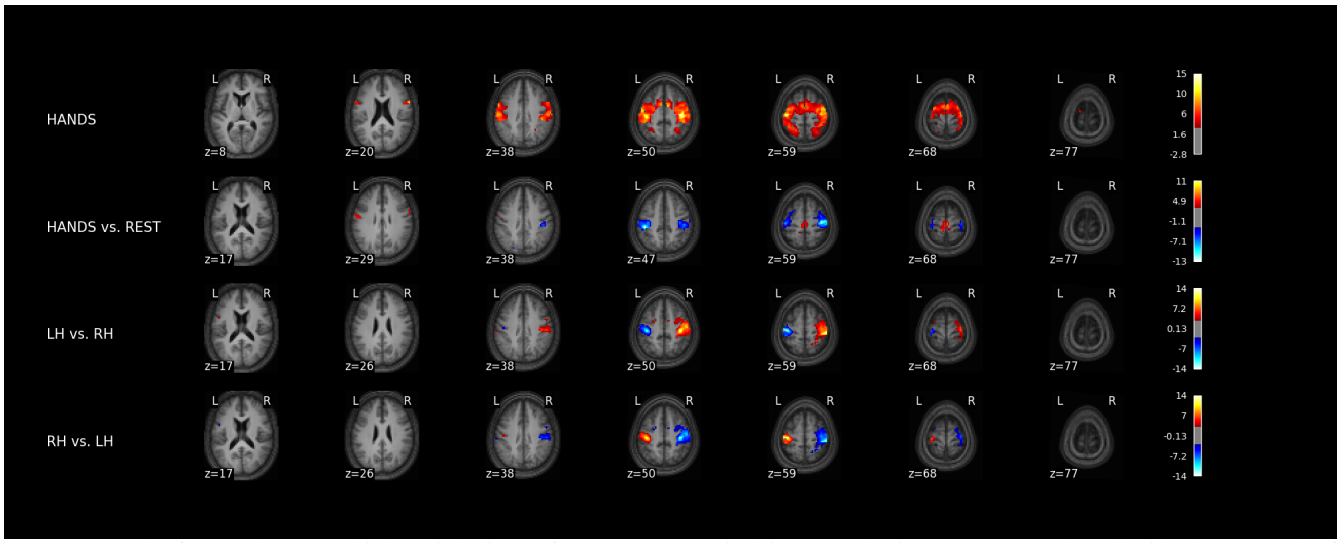

Figure B1. The figure shows multiple axial slices of a mean anatomical image. The images are overlayed with the strength of activations for hand movements in general, hand in contrast with tongue and feet, LH vs. RH and vice-versa. The figure shows that both hand movements activate their contralateral brain region. Moreover, hands are distinctly from feet movements.

Appendix C
Realignment Parameters

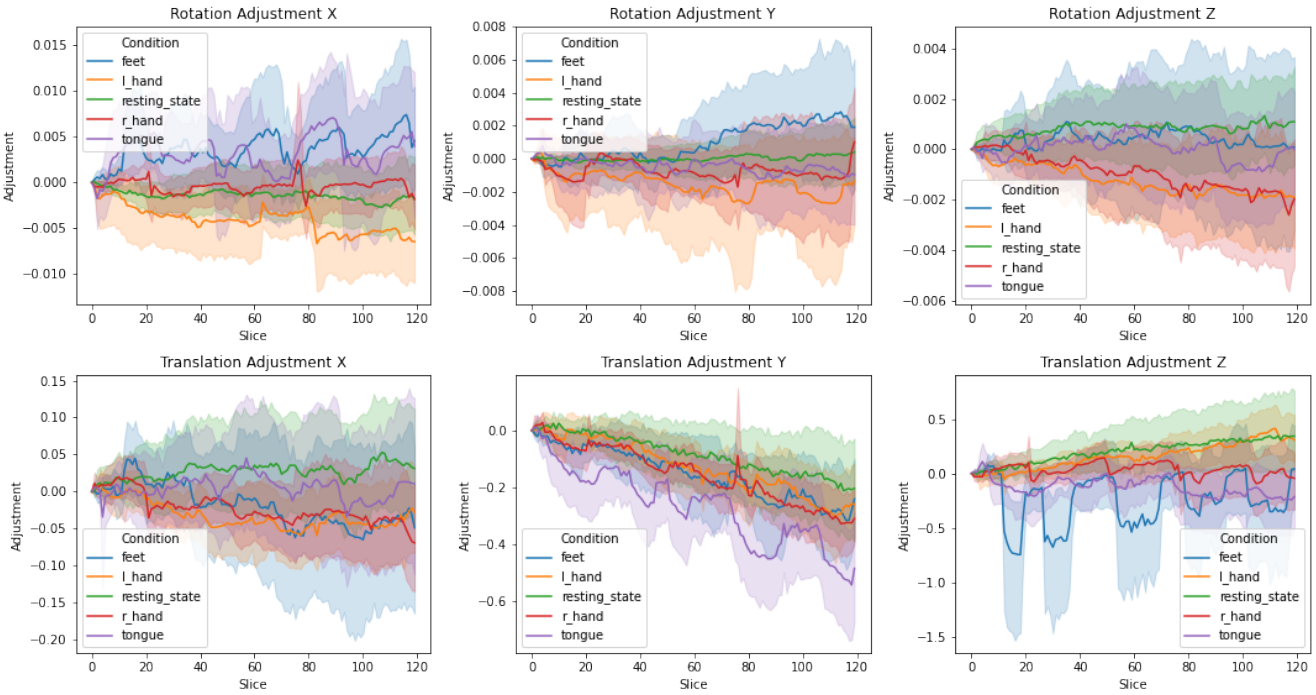

Figure C1. The figure displays the results of the realignment step. The confidence intervals cover 95%. Translations were originally measured in mm and rotations in degrees.

Appendix D
Tongue Movements

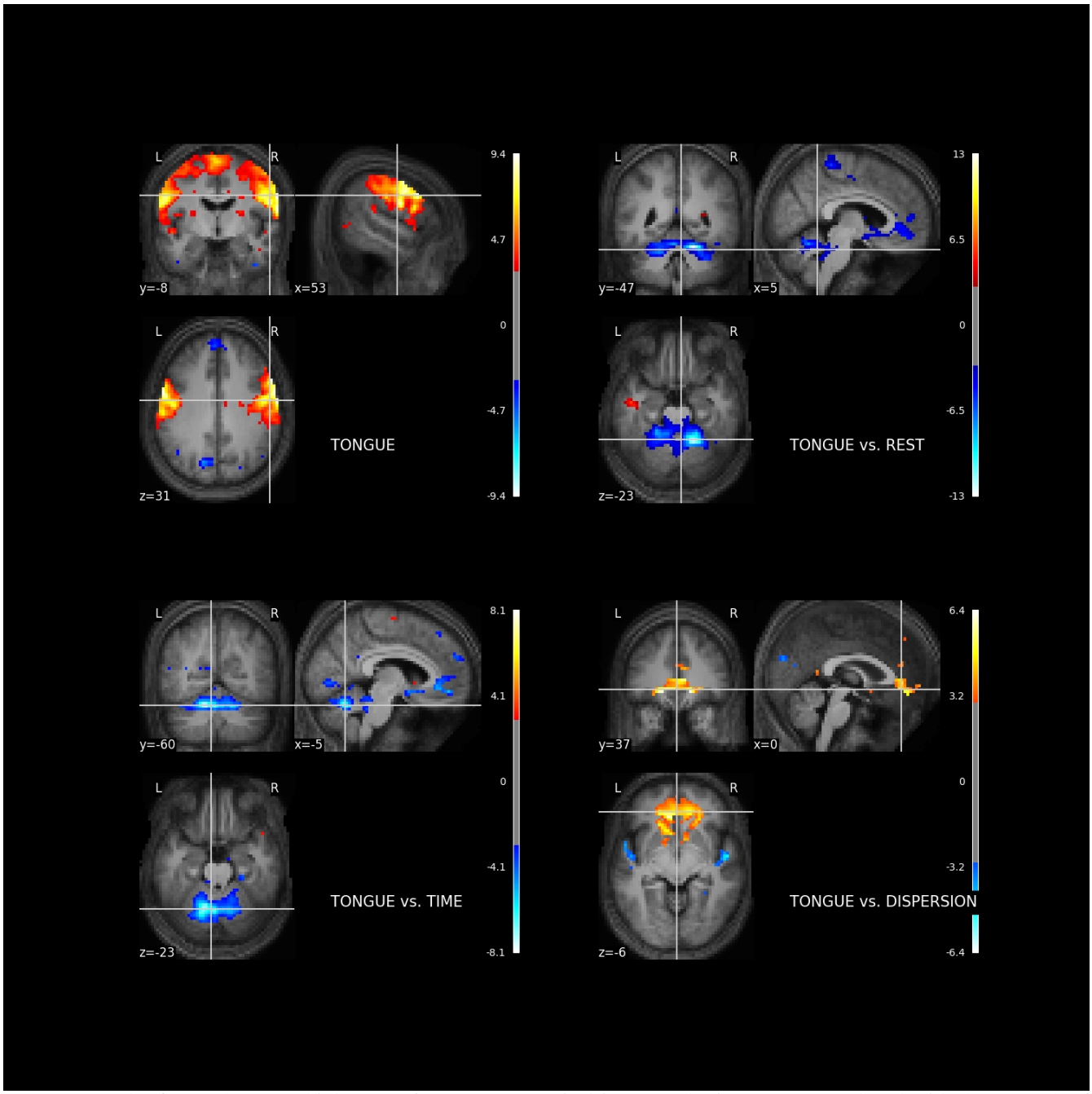

Figure D1. The figure shows multiple cuts of a mean anatomical image. The images are overlayed with the strength of activations for tongue movements contrasted with nothing, the other conditions, time-corrected HRF and dispersion corrected HRF. Furthermore, it shows the activation if no masks are applied.